International Conference on Nuclear Data for Science and Technology 2007
DOI: 10.1051/ndata:07617

Evaluation of the ^{103}Rh neutron cross-section data in the unresolved resonance region for improved criticality safety

L.C. Mihailescu[1,a], I. Sirakov[1], R. Capote[2], A. Borella[1], K.H. Guber[3], S. Kopecky[1], L.C. Leal[3], P. Schillebeeckx[1], P. Siegler[1], E. Soukhovitskii[4], and R. Wynants[1]

[1] European Commission, Joint Research Centre, Institute for Reference Materials and Measurements, 2440 Geel, Belgium
[2] IAEA Nuclear Data Section, Wagramer Strasse 5, 1400 Vienna, Austria
[3] Oak Ridge National Laboratory, P.O. Box 2008, Oak Ridge, TN 37831-6356, USA
[4] Joint Institute for Energy and Nuclear Research, 220109 Minsk-Sosny, Belarus

Abstract. New capture and transmission measurements have been performed at GELINA to improve the neutron induced cross-section data for ^{103}Rh in the resonance region. This contribution refers to the evaluation of the neutron cross-section data of ^{103}Rh in the unresolved resonance region. The capture measurements were done at a 30 m measurement station using C_6D_6 detectors and applying the total energy detection principle in combination with the pulse height weighting technique. The transmission measurements were performed at a 50 m station using ^{6}Li-glass scintillators as neutron detectors. The experimental data have been processed with the AGS code, which includes a full propagation of both correlated and uncorrelated uncertainties. The experimental data are interpreted in terms of average resonance parameters using a generalized single level representation. A link to a dispersive coupled-channel optical model is used for information about the energy dependence of the distant level parameters and the neutron strength functions. This link becomes especially valuable when a dispersive potential as the one derived here is employed after being optimized in a wide energy region. Thus, the consistency between the resonance and the high energy region is ensured.

1 Introduction

Improved capture and total cross-sections for several fission products (i.e. ^{103}Rh, ^{133}Cs, ^{143}Nd, ^{149}Sm, ^{151}Sm, ^{155}Gd and ^{131}Xe) are on the NEA High Priority Nuclear Data Request List [1]. New evaluations for fission products, which include full covariance information, are required to respond to the need for more stringent safety margins; to the tendency to operate present power plants (GEN III and GEN III +) at increased fuel burnup; and for criticality safety of spent fuel transport and storage. Collaboration has been started between the IRMM Geel (Belgium) and the ORNL (USA) with the goal to improve the evaluations for the above mentioned nuclei in the thermal and resonance regions, up to the incident neutron energy corresponding to the threshold of the second inelastic level. ^{103}Rh was the first nucleus investigated and this contribution refers to the evaluation of its neutron cross-section data in the Unresolved Resonance Region (URR) from 6 keV to 94 keV. The upper limit of the energy interval was defined by the threshold of the second inelastic level in ^{103}Rh.

New experimental total and capture cross-sections were needed to solve the discrepancies between the existing experimental data from the literature and to reduce the overall uncertainties. The pulsed white neutron spectrum from GELINA (Geel Linear Accelerator) is an excellent facility for such measurements. GELINA delivers a neutron burst with a full width at half maximum of less than 1 ns, which in combination with fast detectors allow a very good neutron energy resolution.

[a] Presenting author, e-mail: Liviu.Mihailescu@ec.europa.eu

2 Experimental setup and data reduction

The transmission setup was placed at a 50 m flight path length. The neutrons were detected with a Li-glass detector. The sample with a thickness of $4.51 \cdot 10^{-2}$ at/barn was placed at the half distance between the neutron detector and the neutron source in a computer driven sample changer. The data were taken in short cycles with alternate sample-in sample-out configurations. Proportional counters filled with BF_3 were used for monitoring the changes in the integral neutron flux from GELINA. For both transmission and capture measurements the background was deduced from measurements with "black resonance" filters.

The transmission factor, T, was determined from the response of the detectors using the following equation:

$$T = \frac{C'_{in} - B'_{in}}{C'_{out} - B'_{out}} \quad (1)$$

where C stands for the number of counts of the detector and B for the background. The subscript "in" and "out" represent the configurations sample-in and sample-out. The prime means that the number of counts was corrected for the dead time of the acquisition system. In the URR, from 6 keV up to 96 keV, the transmission factor was averaged in energy bins with $\Delta E/E < 30\%$. These energy bins assured both that there is a statistically significant number of unresolved resonances in each energy bin and that $\Delta E/E$ is small enough to have reasonable uncertainties in the calculated cross-sections. The average total cross-section was obtained from the average transmission factor after a correction for the effect of the resonance structure (see also ref. [2]). This correction is

explained by the following equation:

$$\langle T\rangle = e^{-n\langle\sigma_T\rangle}\left[1+\frac{n^2}{2}var(\sigma_T)+\cdots\right] = e^{-n\langle\sigma_T^{uncorrected}\rangle}, \quad (2)$$

where the correction factor for the effect of the resonance structure is represented by the term in the brackets and was calculated with the SESH code [3]. The variance of the total cross-section, $var(\sigma_T)$, equals zero when no resonance structure is present. For thick samples, like the one used in the present transmission measurements, the correction factor for the resonance structure may be significant, reaching a value of about 18% at 5 keV (fig. 1). The experimental setup for the capture measurements was based on C_6D_6 detectors placed at 125° with respect to the neutron beam direction. The total energy principle with the weighting function technique was used for the capture measurements. The neutron flux was permanently monitored with a ^{10}B ionization chamber placed at about 1 m upstream the sample. Two metallic samples were used with a thickness of $3.37 \cdot 10^{-4}$ at/barn and $1.877 \cdot 10^{-3}$ at/barn. Additional measurements with open beam configurations were done for the determination of the background. The weighting functions were determined by MCNP [4] simulations in which a detailed description of the experimental setup was included. The simulation was done for each measured sample. The same threshold on the pulse height spectrum, equal to 150 keV, was considered both in the simulation and in the reduction of the experimental data. The experimental capture yield was calculated using the equation:

$$Y_c = N\cdot\frac{(C'_w - B'_w)}{(E_n + S_n)}\cdot\frac{\sigma_{^{10}B}}{(C'_{IC} - B'_{IC})}, \quad (3)$$

where $\sigma_{^{10}B}$ is the standard cross-section of the reaction ^{10}B(n,α)^{7}Be, E_n is the incident neutron energy and S_n is the neutron binding energy in ^{103}Rh. C and B are the number of counts in the measurement with the sample and in the background respectively. The prime sign stands for the correction for the dead time in the acquisition system. The number of counts in the C_6D_6 detectors were weighted. N is a normalization constant and it was determined in the resolved resonance region using the resonance analysis code REFIT. Several resonances between 100 eV and 300 eV were used to fit the normalization constant. It was observed that for the thin ^{103}Rh sample the normalization constant does not depend on the resonance strength. The resonance parameters of all these resonances were previously determined [5] from a simultaneous fit of capture and transmission data in the energy region from thermal up to 300 eV.

In the URR the capture yield was averaged in energy bins with $\Delta E/E < 30\%$, in the energy interval between 6 keV and 96 keV. The average capture cross-section was corrected for the effect of multiple scattering and self-shielding. The combined correction factor for these effects, C_{ms}, is defined in equation (4). This correction was calculated iteratively with the SESH [3] code. For the thin sample the correction is very small, less than 0.5%. For the thick sample the correction is much higher and detailed investigation still has to be done. Therefore, only the results obtained with the thin sample will be shown here.

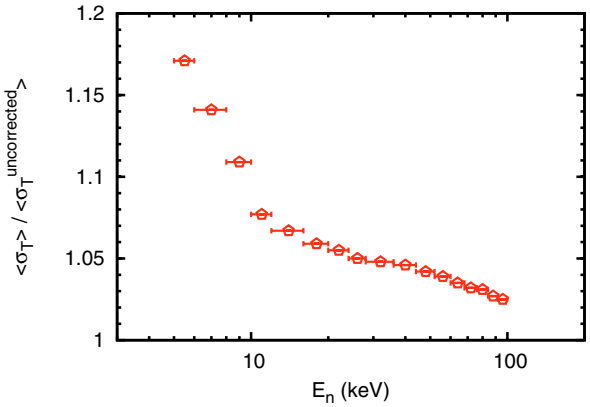

Fig. 1. The calculated ratio between the corrected and the uncorrected average total cross-section. This ratio shows the effect of the resonance structure in the transmission measurements with a sample of $4.51 \cdot 10^{-2}$ at/barn. The calculation was done with SESH code [3].

$$\langle Y_c\rangle = \left\langle\mu\frac{(1-e^{-n\sigma_T})}{n\sigma_T}n\sigma_c\right\rangle = C_{ms}\cdot n\cdot\langle\sigma_c\rangle. \quad (4)$$

3 Data analysis and results in the URR

The average compound partial cross-sections in the URR were expressed in terms of transmission coefficients by applying the Hauser-Fechbach theory with the width fluctuation correction factor in a standard way. In order to represent the non-fluctuating cross-sections, an isospin dependent coupled-channel optical model potential containing a dispersive term with a nonlocal contribution has been derived from fits to the entire neutron and proton scattering data set following a methodology outlined in refs. [6,7]. ^{103}Rh is expected to be a well deformed rigid rotor, where low-lying collective levels are strongly excited in nucleon inelastic scattering. The customary coupled-channels calculations were performed by coupling the first six states of the ground state $K^\pi = 1/2^-$ rotational band up to an excitation energy of 1.41 MeV. The obtained DCCOM potential parameters that show a smooth energy dependence and energy independent geometry are given in the table 1.

A link to the derived DCCOM was used to determine the energy dependence of the potential scattering radius (R′) and of the neutron strength functions [8]. It is noteworthy the fact that dispersive relations guarantee the continuity of the real part of the DCCOM potential from the positive energies (scattering region) to the negative energies (bound states). Furthermore, the link to the optical model ensures that the evaluation in the URR is consistent with the evaluation at higher energies and that no discontinuities appear at the upper energy limit of the URR. The energy dependence of the potential scattering radius and of the strength function was of the order of few percents on the full energy range from 6 keV to 96 keV. The parameters needed to describe the cross-sections were: the potential scattering radius R′, the neutron strength function S_{nl} and the gamma strength function $S_{\gamma l}$ for $l = 0, 1, 2$. The gamma strength function depends on

Table 1. Dispersive coupled-channel OMP parameters for ^{103}Rh with deformation parameters $\beta_2 = 0.191$, $\beta_4 = -0.014$, $\beta_6 = 0.0058$ (RIPL 1479).

	VOLUME	**SURFACE**	**SPIN-ORBIT**
Real depth [MeV]	$V_0 = 49.73$ $\lambda_{HF} = 0.0091$ $C_{viso} = 10.0$ + dispersive ΔV_V	dispersive ΔV_S	$V_{so} = 4.46$ $\lambda_{so} = 0.005$ + dispersive ΔV_{SO}
Imaginary depth [MeV]	$A_v = 12.14$ $B_v = 82.17$ $E_a = 165$	$W_0 = 13.94$ $B_s = 11.77$ $C_s = 0.007933$ $C_{wiso} = 23.5$	$W_{so} = -3.1$ $B_{so} = 160$
Geometry [fm]	$r_{HF} = 1.2499$ $a_{HF} = 0.637$ $r_v = 1.037$ $a_v = 0.699$	$r_s = 1.2318$ $a_s = 0.563$	$r_{so} = 1.1294$ $a_{so} = 0.59$

Table 2. The average resonance parameters resulted from the present fit compared with the other evaluations. The values of the parameters marked with * were deduced from the resolved resonance region and they were fixed in the present fit.

R′(fm)($E_n = 0$)	D_0 (eV)	S_l ($E_n = 0$) (10^{-4})			$\langle\Gamma_\gamma\rangle_l$ (meV)			$S_{\gamma 0}$ (10^{-3})	Reference
		$l = 0$	$l = 1$	$l = 2$	$l = 0$	$l = 1$	$l = 2$		
6.44	23.14	0.60	4.60	0.61	165.0*	123.4	165.0*	7.13	This work
6.56	28.60	0.57	4.81	1.00	170.0	150.0	140.0	5.94	ENDF B-VII
6.51	26.00	0.58	4.21	0.63	172.0	160.0	172.0	6.61	JEFF 3.1
6.52	32.13	0.44	4.10	0.53	230.0	230.0	230.0	9.96	JENDL 3.2 (3.5 keV)

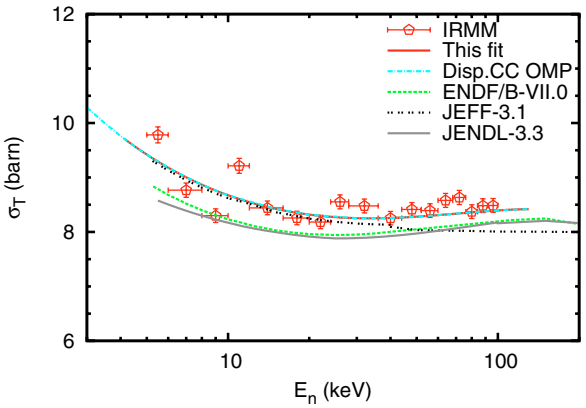

Fig. 2. The average neutron total cross-section of ^{103}Rh in the URR.

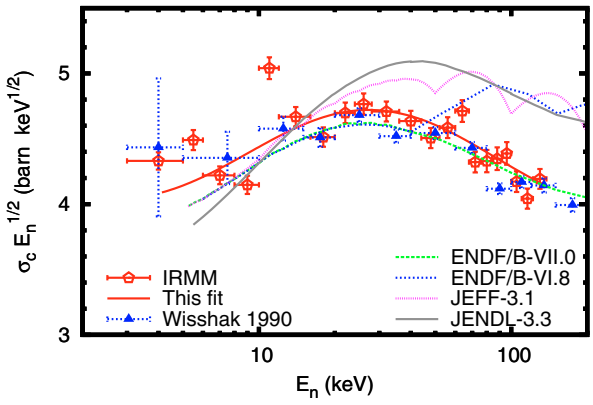

Fig. 3. The average capture cross-section of ^{103}Rh in the URR.

both the average gamma width $\langle\Gamma_{\gamma l}\rangle$ and the average level spacing D_l, where $l = 0, 1, 2$. Therefore, a simultaneous fit of $\langle\Gamma_{\gamma l}\rangle$ and D_l is not recommended because of their strong correlation. A much better approach is to use the available prior information on one of the above mentioned parameters (ex. from the resolved resonance region). In the present fit the average gamma width for the *s*-wave and *d*-wave was assumed constant with a value $\langle\Gamma_{\gamma 0}\rangle = \langle\Gamma_{\gamma 2}\rangle = 165$ meV based on the values from the resolved resonance region. The average resonance parameters that resulted from the present fit are compared in table 2 with the parameters given in the current evaluations, while the calculated cross-sections are compared in figures 2 and 3.

In figure 2, the derived average total cross-section is compared with the other evaluations. The average total cross-section corresponding to the above presented DCCOM potential was calculated using the current version of the EMPIRE system [9,10] and is also shown in the figure. The DCCOM potential fit included the new measured total cross-section obtained in this work, therefore it was no need to fit the neutron strength functions for ^{103}Rh, as long as they are already calculated by the optical model. The new values obtained for the average total cross-section, both experiment and fit, are slightly higher than the ENDF/B-VII.0 and JENDL-3.3 (fig. 2) and agree very well with the JEFF-3.1 evaluation up to about 40 keV, where a discontinuity appears in the latter.

Figure 3 shows the average capture cross-section obtained in this work for ^{103}Rh in comparison with some of the existing evaluations and with the experimental values from Wisshak et al. [11]. Only the data of Wisshak et al. are shown because they were obtained with a thin sample comparable with the one used in this experiment. The two experimental data sets agree very well and moreover their quality is supported by the fact that two complementary methods were used: total energy principle for the GELINA experiment and the total absorption principle for the Wisshak et al. [11] experiment. For the capture channel, the present fit included only the new data from GELINA with the very thin sample. The new evaluation lies between the other evaluations. At energies around 100 keV the new evaluation tends to be closer to the ENDF/B-VII.0.

4 Conclusions

New capture and transmission measurements were done at GELINA for ^{103}Rh and preliminary results in the unresolved resonance region were shown here. These new measurements completed a set of measurements at GELINA such that the full energy range from thermal up to the threshold of the second inelastic level was covered using a combination of different flight path lengths and samples thicknesses. Because of its high thermal cross-section ^{103}Rh is an example of a nucleus for which the full energy range from thermal up to the threshold of the second inelastic level can be covered at GELINA.

The average resonance parameters (neutron and gamma strength functions and the potential scattering radius) were extracted from the fit of the experimental data. For the total cross-sections all the data from the literature were used in the fit, while for the capture channel only the present data with the thin sample were used.

All these new measurements together with the existing measurements from the literature will be used in a new evaluation of the cross sections, in ENDF-6 format, from the thermal energy up to about 100 keV. A detailed investigation of the uncertainties is planned including the generation of the full covariance matrix.

The authors are grateful to the GELINA operators for the dedicated and skillful running of the accelerator.

References

1. F. Storrer, P. Bioux, D. Biron, D. Hittner, J. Palau, B. Roque, J. Ruggieri, A. Santamarina, H. Toubon, C. Traka et al., *Priority nuclear data needs for industrial applications*, in *ND2001*, J. Nucl. Sci. Technol. Suppl. 2,1357 (2002).
2. A. Borella, K. Volev, A. Brusegan, P. Schillebeeckx, F. Corvi, N. Koyumdjieva, N. Janeva, A. Lukyanov, Nucl. Sci. Eng. **152**, 1 (2006).
3. F. Frohner, *SESH – A Fortran IV code for calculating the self-shielding and multiple scattering effects for neutron cross-section data interpretation in the unresolved resonance region*, GA-8380, Gulf General Atomic (1968).
4. J.F. Briesmeister, *MCNP*^{TM} *– A General Monte Carlo N-Particle Transport Code*, Report LA-13709-M, Los Alamos National Laboratory, Los Alamos NM, USA (2000).
5. A. Brusegan, E. Berthoumieux, A. Borella, F. Gunsing, M. Moxon, P. Siegler, P. Schillebeeckx, in *Proceedings of the International Conference on Nuclear Data for Science and Technology, 27 Sept.–1 Oct. 2004, Santa Fe, NM, USA.*; AIP Conf. Proc. **769**, 953 (2005).
6. E.S. Soukhovitskii, R. Capote, J.M. Quesada, S. Chiba, Phys. Rev. C **72**, 024604 (2005).
7. R. Capote, E.S. Soukhovitskii, J.M. Quesada, S. Chiba, Phys. Rev. C **72**, 064610 (2005).
8. I. Sirakov, P. Schillebeeckx, R. Capote, *Evaluation of neutron cross section data in the unresolved resonance region with a link to the optical model*, in *Proc. of Workshop On Nuclear Data Evaluation for Reactor applications-WONDER 2006* (2006).
9. R. Capote, M. Sin, A. Trkov, M. Herman, B.V. Carlson, P. Obložinsk, *Extension of the nuclear reaction model code EMPIRE to actinides nuclear data evaluation* (these proceedings).
10. M. Herman, P. Obložinsky, R. Capote, M. Sin, A. Trkov, A. Ventura, V. Zerkin, in *Proceedings of the International Conference on Nuclear Data for Science and Technology, 27 Sept.–1 Oct. 2004, Santa Fe, NM, USA.*; AIP Conf. Proc. **769**, 1184 (2005). Online at http://www.nndc.bnl.gov/empire219/.
11. K. Wisshak, F. Voss, F. Kappeler, G. Reffo, Phys. Rev. C **42**, 1731 (1990).